



Comparative studies of thermogels in preventing post-operative adhesions and corresponding mechanisms

Journal:	<i>Biomaterials Science</i>
Manuscript ID:	BM-ART-01-2014-000029.R1
Article Type:	Paper
Date Submitted by the Author:	12-Feb-2014
Complete List of Authors:	<p>Yu, Lin; Fudan University, Dept. of Macromolecular Science Hu, Hongtao; Changzheng Hospital, Second Military Medical University of the Chinese People's Liberation Army, Department of Orthopedic surgery Chen, Lin; Fudan University, Dept. of Macromolecular Science Bao, Xiaogang; Changzheng Hospital, Second Military Medical University of the Chinese People's Liberation Army, Department of Orthopedic surgery Li, Yuzhuo; Fudan University, Dept. of Macromolecular Science Chen, Liang; Fudan University, Dept. of Macromolecular Science Xu, Guohua; Changzheng Hospital, Second Military Medical University of the Chinese People's Liberation Army, Department of Orthopedic surgery Ye, Xiaojian; Changzheng Hospital, Second Military Medical University of the Chinese People's Liberation Army, Department of Orthopedic surgery Ding, Jiandong; Fudan University, Key Lab of Macromolecular Engineering of Polymers of Chinese Ministry of Education, Dept. of Macromolecular Science</p>

Comparative studies of thermogels in preventing post-operative adhesions and corresponding mechanisms

Lin Yu^{a,1}, Hongtao Hu^{b,1}, Lin Chen^a, Xiaogang Bao^b, Yuzhuo Li^a, Liang Chen^a,

Guohua Xu^{b,}, Xiaojian Ye^b, Jiandong Ding^{a,*}*

^a *State Key Laboratory of Molecular Engineering of Polymers, Department of Macromolecular Science, Fudan University, Shanghai 200433, China*

^b *Department of Orthopedic Surgery, Changzheng Hospital, Second Military Medical University of the Chinese People's Liberation Army, Shanghai 200003, China*

¹ The two authors contributed equally.

* Corresponding authors, Tel: +86-21-65643506; fax: +86-21-65640293

E-mail address: xuguohuamail@163.com (G.H. Xu) or jdding1@fudan.edu.cn (J.D. Ding)

Abstract: Post-surgical peritoneal adhesions constitute a classic problem in surgery, and thus anti-adhesion materials are much required. In this study, a series of polyester-PEG-polyester triblock copolymers with different biodegradable polyester compositions were synthesized; their properties were examined, and the *in vivo* efficacies as anti-adhesion biomaterials were evaluated in a comparative way for the first time. These samples not only exhibited various morphologies at the bulk state, but also possessed different stabilities at the sol state. All the polymer aqueous solutions with appropriate compositions and concentrations underwent sol-gel transitions with increase of temperature and formed semi-solid hydrogels at the body temperature. The efficacy of PEG/polyester thermogels (25 wt%) on preventing post-operative abdominal adhesions was investigated and compared in a rabbit model of sidewall defect-bowel abrasion. Different efficacies of anti-adhesions were observed; possible mechanisms were discussed, and the importance of viscoelasticity was suggested for the first time. These results illustrated that appropriate properties of PEG/polyester thermogels including viscoelastic matrix, hydrophilic surface and moderate *in vivo* persistence played crucial roles to enable an effective device to prevent post-surgical peritoneal adhesions.

Keywords: Post-operative adhesions, thermogel, PEG, biodegradable polyester, barrier device

Introduction

One of the common and serious complications in surgery is the formation of post-operative peritoneal adhesions, which can cause a series of secondary diseases such as severe pain, infertility, intestinal obstruction and even death.¹⁻³ Incidence of adhesions is as high as 80% after general surgical procedures.³ Especially, almost all patients suffer from intestinal adhesions after abdominal and pelvic surgery.⁴ Post-operative adhesions affect millions of individual in the world, and induce billions of expense in re-operative interventions.

Over the past decades, numerous pharmacological and barrier-based approaches have been tried to prevent post-operative adhesions.⁵⁻⁸ The barrier systems in the form of polymer solutions or solid membranes are currently one of the most effective approaches for reducing adhesion formation.⁹⁻¹² They separate the injured regions during the critical period of adhesion development at 3-5 days after surgery. This separation is achieved via the hydroflotation effect of polymer solutions or the directly physical isolation with the use of solid membranes. For polymer solutions such as chitosan, hyaluronic acid (HA) and carboxymethylcellulose (CMC),^{9, 10} the residual time at the injured tissues is short; for solid membranes including HA-CMC (Seprafilm, Genzyme, Cambridge, MA) and polylactide,¹³⁻¹⁵ they are difficult to completely cover the affected tissues.

Recently, in situ-forming hydrogels have been developed as injectable biomaterials for drug delivery,¹⁶⁻²² tissue repairing²³⁻²⁵ and submucosal injection substance in endoscopic submucosal dissection,^{26, 27} and other biomedical applications.^{28, 29} Such a

class of biomaterials is a low-viscous sol before administration and turns into a semi-solid gel under the physiological condition once being injected into the target site. Meanwhile, these materials offer the ability to form any desired implant shape, and the use of organic solvents in operation is completely avoided. Some in situ chemically cross-linked hydrogels based on HA,^{30, 31} dextran,³² gelatin¹¹ or macromonomers of poly(ethylene glycol) (PEG)³³ have been applied for preventing the formation of post-operative peritoneal adhesion. Nevertheless, in situ gelation triggered by chemical modification or cumbersome ultraviolet (UV) illumination may bring with some biocompatibility problems, and the relative long gelation time also restricts the practically clinical applications. In situ physically crosslinked hydrogels have become an alternative choice.^{4, 8, 34-36} For example, Guardix-SG (Biorane, Seoul, Korea) is a temperature-sensitive physical gel consisting of Pluronics/Alginate/CaCl₂ and has successfully prevented pericardial adhesion in a rabbit model.³⁶

As a unique injectable physical hydrogel, thermogels have gained increasing attention recently. Some amphiphilic block copolymers are not only dissolved in water at low or room temperature, but also undergo, under appropriate composition and concentration, a reversible sol-gel transition upon heating, as illustrated in **Fig. 1a**, and thus called thermogel.³⁷⁻⁴² Thermogelling copolymers composed of PEG and aliphatic polyesters are particularly interesting and important, because both blocks have been approved by US Food and Drug Administration (FDA). To date, a variety of biodegradable polyester chains such as poly(D,L-lactic acid-*co*-glycolic acid) (PLGA),⁴³⁻⁴⁶ poly(ϵ -caprolactone) (PCL),^{47, 48} poly(ϵ -caprolactone-*co*-D,L-lactic

acid) (PCLA),^{49, 50} and poly(ϵ -caprolactone-*co*-D,L-lactic acid) (PCGA),⁵¹ have been introduced as the hydrophobic blocks into PEG/polyester copolymers to form thermogels. The basic mechanism of the thermogelation of PEG/polyester copolymers is the formation of a percolated micelle network.^{40, 52, 53}

In 2011, our group suggested and confirmed that the biodegradable and thermoreversible PCLA-PEG-PCLA hydrogel could serve as a physical barrier for prevention of post-operative adhesions,⁵⁴ and thus an important and facile medical application of such a kind of interesting soft matters was explored. As a result, a series of fundamental questions are triggered. For instance, is the thermogel with the most popular composition, namely, PLGA-PEG-PLGA, feasible as an anti-adhesion biomaterial? Do viscoelastic properties and biodegradable periods of thermogels with different polyester compositions influence the *in vivo* efficacy of prevention of post-operative adhesions? Answering of these questions should be based upon much work, and the corresponding efforts are meaningful for guiding the potential medical applications of the thermogels.

Herein, three thermogelling ABA-type PEG/polyester triblock copolymers with commonly used polyester compositions were synthesized. **Fig. 1b** shows the molecular structures of the three PEG/polyester triblock copolymers synthesized in this study. We selected the three compositions based upon the following considerations. PLGA has been clinically applied and widely investigated as biomaterials. PLGA-PEG-PLGA thermogels have also been extensively studied by several groups,^{38, 44, 55} yet it has never been reported as a barrier device for

post-operative anti-adhesions. Hence, it seems necessary to examine the feasibility of PLGA-PEG-PLGA thermogels. PCL-PEG-PCL is a typical thermogel with a crystal structure.⁴⁷ Yet again its feasibility as an anti-adhesion biomaterial has not been examined. Recently, based on molecular parameter design, our group achieved the block copolymers of PCGA-PEG-PCGA with a powder form at dry state and a temperature-induced sol-gel transition in water without unexpected gelling prior to heating.⁵¹ Therefore, we would like to examine this system together with PLGA-PEG-PLGA and PCL-PEG-PCL. These samples have been proved to be biocompatible and biodegradable.⁵⁵⁻⁵⁸ Their different viscoelasticities and degradation rates have also been reported.^{47, 51, 57, 59} The novelty of the present study is to evaluate the efficacy of prevention of post-surgical tissue adhesions with the use of these thermogels for the first time and shed some insights to design a thermogel-based barrier system for post-surgical anti-adhesions. Meanwhile, the thermogelling properties of these copolymers have also been investigated together in a comparative way for the first time.

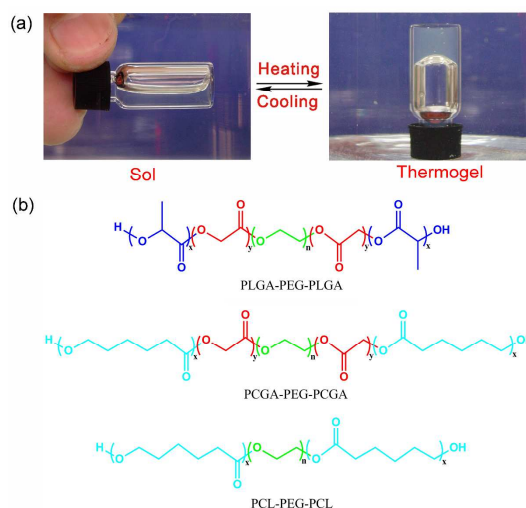


Fig. 1. (a) Schematic presentation of temperature-induced reversible sol-thermogel

transition. (b) The molecular structures of three thermogelling block copolymers composed of polyester and polyether, PLGA-PEG-PLGA, PCGA-PEG-PCGA, and PCL-PEG-PCL.

Materials and methods

Materials

DL-lactide (LA, Purac), glycolide (GA, Purac), ϵ -Caprolactone (CL, Aldrich), stannous octoate (Aldrich), and PEG with molecular weight (MW) 1500 (Aldrich) were used as received without further purification. Medical chitosan (CHS) was provided by Shanghai Qisheng Biological Fabrication Co., Ltd, China.

Animals

Male New Zealand rabbits with body weight 2.0 ± 0.2 kg were supplied by the Experimental Animal Center of the Second Military Medical University of the Chinese People's Liberation Army (SMMU, Shanghai, China). The animals were raised at a temperature of 25 ± 2 °C and a relative humidity of $70 \pm 5\%$ with cycles of 12 h light and 12 h dark at least for 1 week before experiment. All the animal experiments were conducted with approval from the ethics committee of Changzheng Hospital for animal investigation.

Synthesis of polyester-PEG-polyester triblock copolymers

The ABA-type PEG/polyester triblock copolymers were synthesized via bulk ring-opening polymerization. The detailed procedure has been described elsewhere.⁴⁶

⁶⁰ To synthesize the PLGA-PEG-PLGA, PEG (20 g) was added into a three-necked

flask and heated under vacuum at 150 °C for 3 h. Next, GA and LA monomers were added after the flask was cooled to room temperature. The replacement of argon in the flask was carried out three times to eliminate the residual moisture in monomers. Then, the reaction system was heated under an argon atmosphere at 150 °C for 12 h after the addition of stannous octoate (0.2 wt% of monomers). Crude polymers were washed using 80 °C hot water at least for three times. The residual water was removed via lyophilization and the final products were stored at -20 °C refrigerator until use. The other two specimens PCGA-PEG-PCGA and PCL-PEG-PCL were prepared with a similar procedure but different monomers.

¹H NMR characterization

¹H NMR spectra were recorded at ambient temperature with a Bruker spectrometer (DMX500) operating at 500 MHz to study chemical structure and composition of the polymers. CDCl₃ was used as the solvent, and chemical shifts (δ) were given in ppm using tetramethylsilane as internal standard.

Gel permeation chromatography

Gel Permeation Chromatography (GPC) measurements were performed on an Agilent apparatus (Agilent1100) equipped with a refractive index detector. Tetrahydrofuran was used as the mobile phase at a flow rate of 1.0 mL/min at 35 °C. A 1.0% (w/v) polymer solution (20 μL) was injected for per analysis. MWs were calibrated by monodispersed polystyrene standards.

Differential scanning calorimetry

A differential scanning calorimeter (DSC Q2000, TA) was used to measure the

melting and crystallization temperatures of the polymers in the temperature ranging from -20 to 80 °C. 5.0 mg of polymer was loaded in a cell for each analysis and DSC thermograms were registered with a heating and cooling rate of 5 °C/min.

X-ray diffraction analysis

X-ray diffraction (XRD) was performed using a PANalytical X'Pert PRO diffractometer equipped with a Cu K α radiation source. The diffraction patterns of a scan range between 5° to 50° were recorded with a scanning rate of 5 °/min at room temperature. The voltage was set at 40 KV and the current was fixed at 40 mA.

Rheological measurements

A stress-controlled rheometer (Malvern, Kinexus) equipped with a 60 mm steel cone (1 degree) using a gap size of 0.03 mm was used to study the sol-gel transition of polymer aqueous solution as the temperature increased. Solutions of 25 wt % copolymer in normal saline solution (NS) were transferred onto the rheometer. In stress-controlled dynamic rheological measurements, a sinusoidal shear stress with a given frequency ω was exerted on the sample, and the corresponding time-dependent shear strain was detected. We controlled small oscillatory amplitudes to guarantee the range of the linear viscoelasticity, and thus the shear strain was also changed sinusoidally but probably with a phase different from that of the shear stress if the material is not fully elastic. The plate was heated at a rate of 0.5 °C/min and the oscillatory frequency ω was fixed at 10 rad/s. The viscoelastic properties of the polymer aqueous solutions, namely, the dynamic shear storage modulus (G') and loss or dissipative modulus (G'') were recorded as a function of temperature. The complex

modulus (G^*) was determined based on the equation $G^* = \sqrt{G'^2 + G''^2}$, and the phase angle δ was obtained via $\tan\delta = G''/G'$.

***In vivo* anti-adhesion tests**

A rabbit model of sidewall defect-bowel abrasion^{30, 31} was used to evaluate the anti-adhesion efficacy of the PEG/polyester thermogels with different polyester blocks. Briefly, after anesthetizing the animal with 3% sodium pentobarbital solution, the enterocoelia was opened. A 3×4 cm² defect on the right lateral abdominal wall was created and the corresponding cecal haustra was abraded using a surgical brush. And thus a model of peritoneal intestinal adhesion was established.

The rabbits were randomly divided into five groups (six per group): Control (without treatment), PLGA-PEG-PLGA (4 mL of the PLGA-PEG-PLGA solution (25 wt% in NS) was pipetted onto the defects, and spontaneous gelation happened rapidly due to contacting the warmer surroundings), PCGA-PEG-PCGA (administration of 4 mL of the PCGA-PEG-PCGA solution), PCL-PEG-PCL (administration of 4 mL of the PCL-PEG-PCL solution), CHS (administration of 4 mL of the biomedical chitosan solution). Finally, the peritoneum and abdominal wall were sutured using 3-0 silk sutures, and the skin was sutured using 4-0 silk sutures.

The rabbits were euthanized 30 days after surgery. The autopsy was performed to assess the post-operative adhesion and the tissue regeneration on defect. If intestinal adhesion occurred, the adhesion area of the sidewall injury was measured. The tenacity of the intestinal adhesion found was also defined as follows: score 0: no adhesion; score 1: mild intestinal adhesion and separation was facile; score 2:

moderate intestinal adhesion and blunt dissection was needed; score 3: severe intestinal adhesion and sharp dissection was needed. Specimens were harvested, fixed in 10 % formalin, embedded in paraffin, and cut into slices of thickness 4 μm . The sections were routinely stained with haematoxylin-eosin (HE) and observed with a light microscope.

Results

Synthesis and characterization of polyester-PEG-polyester triblock copolymers

Three polyester-PEG-polyester triblock copolymers were prepared via the ring-opening polymerization of different monomers in the presence of α,ω -dihydroxyl terminated PEG using stannous octoate as catalyst. Typical ^1H NMR spectra of the triblock copolymers with their chemical structures are presented in **Fig. 2**. All the characteristic signals are assigned on the spectra. For PLGA-PEG-PLGA, the peaks at 5.20 ppm ($-\text{COCH}(\text{CH}_3)\text{O}-$), 4.80 ppm ($-\text{COCH}_2\text{O}-$) and 3.65 ppm ($-\text{CH}_2\text{CH}_2\text{O}-$) were used to calculate the number-average MW (M_n).⁴⁰ In the case of PCGA-PEG-PCGA and PCL-PEG-PCL, the peaks around 4.60 ppm ($-\text{COCH}_2\text{O}-$), 3.65 ppm ($-\text{CH}_2\text{CH}_2\text{O}-$) and 1.39 ppm ($-\text{COCH}_2\text{CH}_2\text{CH}_2\text{CH}_2\text{CH}_2\text{O}-$) were used to determine M_n .^{47, 51} The obtained results are summed in Table 1.

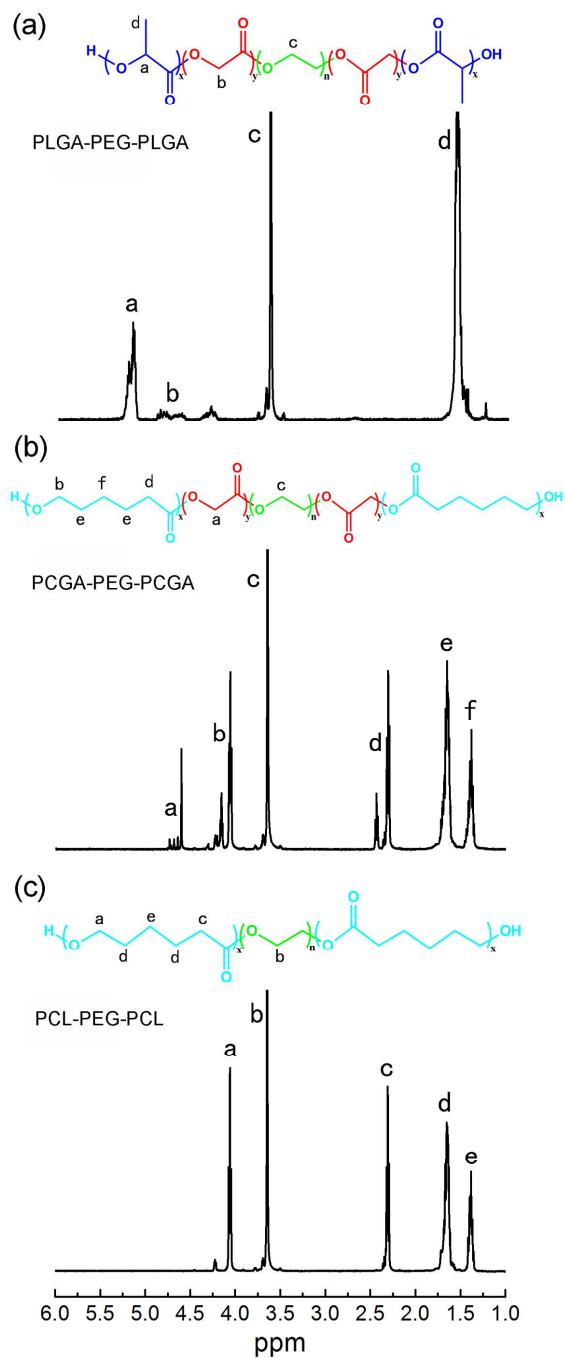


Fig. 2. ^1H NMR spectra of triblock copolymers in CDCl_3 (a) PLGA-PEG-PLGA, (b) PCGA-PEG-PCGA, (c) PCL-PEG-PCL.

The triblock copolymers were further measured via GPC to determine MWs and

their distributions. **Fig. 3** displays the results of GPC analysis. A symmetric peak with a relative narrow MW distribution was observed. The polydispersity index defined as weight-average MW over number-average MW (M_w/M_n) was lower than 1.3 for all of the specimens. Such a result indicated that purity was sufficiently high to investigate their physical-chemical properties. All the quantitative data on M_n and polydispersity index of the copolymers obtained from GPC are also listed in Table 1.

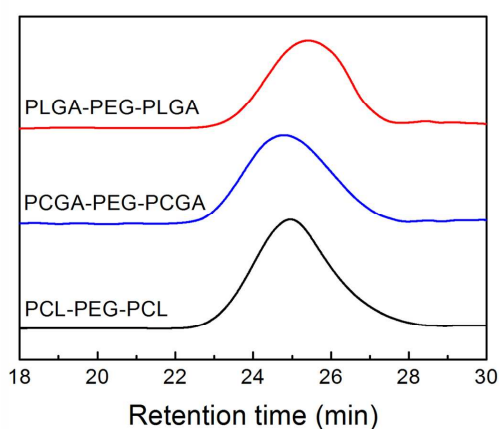


Fig. 3. GPC traces of the indicated triblock copolymers.

Table 1. Characterization of polyester-PEG-polyester triblock copolymers synthesized in this study

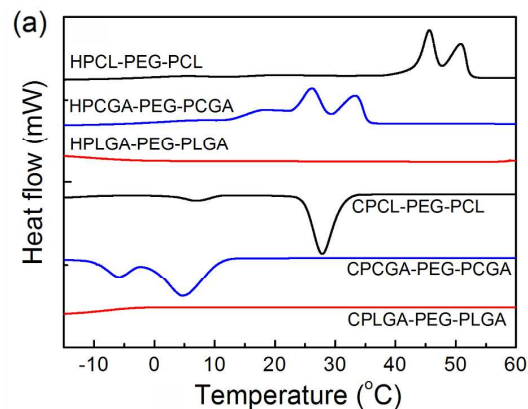
Sample ID	M_n^a	Monomer ratio (mol/mol) ^a	M_n^b	$(M_w/M_n)^b$	Morphology
PLGA-PEG-PLGA	1675-1500-1675	LA/GA = 10/1	6520	1.23	sticky paste
PCGA-PEG-PCGA	1725-1500-1725	CL/GA = 10/1	7570	1.27	powder
PCL-PEG-PCL	1510-1500-1510	/	6980	1.26	powder

^a) The number-averaged MW, M_n of the central block PEG was provided by Aldrich, and M_n of each polyester block was calculated by ¹H-NMR. ^b) Measured

via GPC.

Thermal properties of polyester-PEG-polyester triblock copolymers at the bulk state and the stability of their aqueous solutions

The thermal properties of synthesized copolymers were examined via DSC characterizations. **Fig. 4a** shows DSC thermograms of polyester-PEG-polyester triblock copolymers with various polyester compositions. PCL-PEG-PCL showed two melting transitions at 46 °C and 51 °C in the heating curve and also two crystallization peaks at 7 °C and 28 °C in the cooling curve, which were attributed to the blocks of PCL and PEG, respectively.⁴⁷ Due to the incorporation of GA into PCL block, the crystallization of both PCL and PEG blocks in PCGA-PEG-PCGA was interrupted. Consequently, the melting and crystallization peaks of PCGA-PEG-PCGA were shifted to low temperatures. For PLGA-PEG-PLGA, neither melting peak nor crystallization peak was detected during the heating and cooling cycles, suggesting that the polymer exhibits an amorphous state.



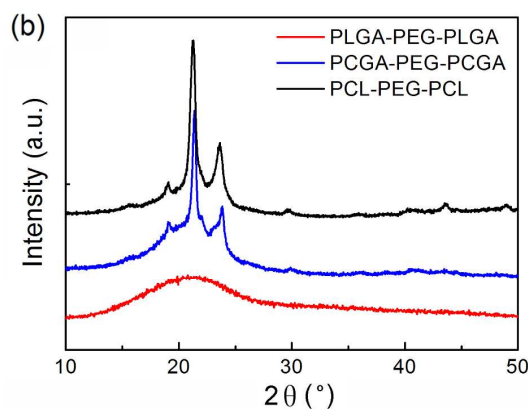


Fig. 4. (a) DSC thermograms of the indicated triblock copolymers in the second heating run and the first cooling run. HPLGA-PEG-PLGA, HPCGA-PEG-PCGA, HPCL-PEG-PCL indicate heating curves, while CPLGA-PEG-PLGA, CPCGA-PEG-PCGA, CPCL-PEG-PCL refer to cooling curves. The heating and cooling rate was 5 °C/min. (b) XRD patterns of the indicated triblock copolymers.

The crystalline or amorphous behavior of three triblock copolymers was further analyzed via XRD measurements. **Fig. 4b** shows their XRD patterns. In the case of PCL-PEG-PCL, two strong diffraction peaks at 21.2° and 23.8° were observed, which came from the crystallization of the PCL component.⁵¹ PCGA-PEG-PCGA presented a similar pattern to PCL-PEG-PCL. The XRD pattern of PLGA-PEG-PLGA just exhibited a broad amorphous peak. These features coincided with the DSC results.

The three samples had different morphologies as a neat polymer. PLGA-PEG-PLGA presented a sticky paste at the bulk state, while the other two samples had a powder form, as shown in **Fig. 5a**. Different from sticky PLGA-PEG-PLGA, powder PCGA-PEG-PCGA and PCL-PEG-PCL allowed comfortable handling in weighing and transferring, and meanwhile different

approaches were used to prepare their aqueous solutions. PLGA-PEG-PLGA was dissolved in water using stirring at low or room temperature and several hours were needed. The aqueous solution of PCGA-PEG-PCGA was easily prepared by heating the polymer/water system at 55 °C for several minutes followed by quenching in an ice bath for 30 min. The PCL-PEG-PCL aqueous solution was obtained via a similar method but using a higher temperature (70 °C) to melt the polymers. Moreover, the varying stabilities of their aqueous solutions at ambient temperature were observed. When the aqueous solution of PCL-PEG-PCL was left at room temperature (20 °C) for one hour, an opaque gel was spontaneously formed, which was attributed to the crystallization of PCL.⁵¹ In contrast, the aqueous solutions of the other two samples maintained their sol states at the same condition with the results displayed in **Fig. 5b**.

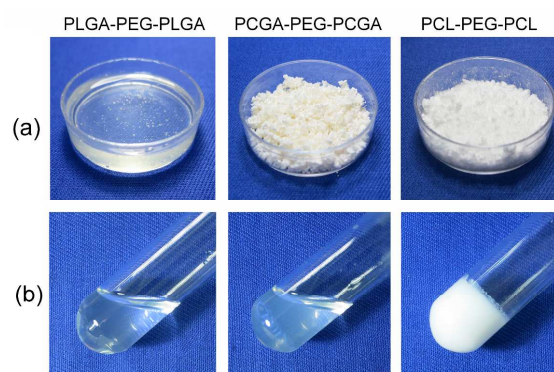


Fig. 5. (a) Bulk morphologies of the indicated triblock copolymers. (b) The stability of their aqueous solutions. PLGA-PEG-PLGA and PCGA-PEG-PCGA systems maintained the stable sols, while PCL-PEG-PCL spontaneously formed a crystal gel when their aqueous solutions were stored at room temperature for one hour.

Sol-gel transition of polyester-PEG-polyester triblock copolymers in water

All the polyester-PEG-polyester triblock copolymers in sol state were free-flowing liquids and exhibited a sol-gel transition in response to an increase of temperature. The sol-gel transitions of their aqueous solutions (25 wt% in NS) as a function of temperature were quantitatively evaluated using a stress-controlled rheometer with the results shown in **Fig. 6a-d**. The storage modulus G' , loss modulus G'' , complex modulus G^* and phase angle δ of the polymeric aqueous systems abruptly changed as the temperature increased, indicating the formation of in situ thermogels.

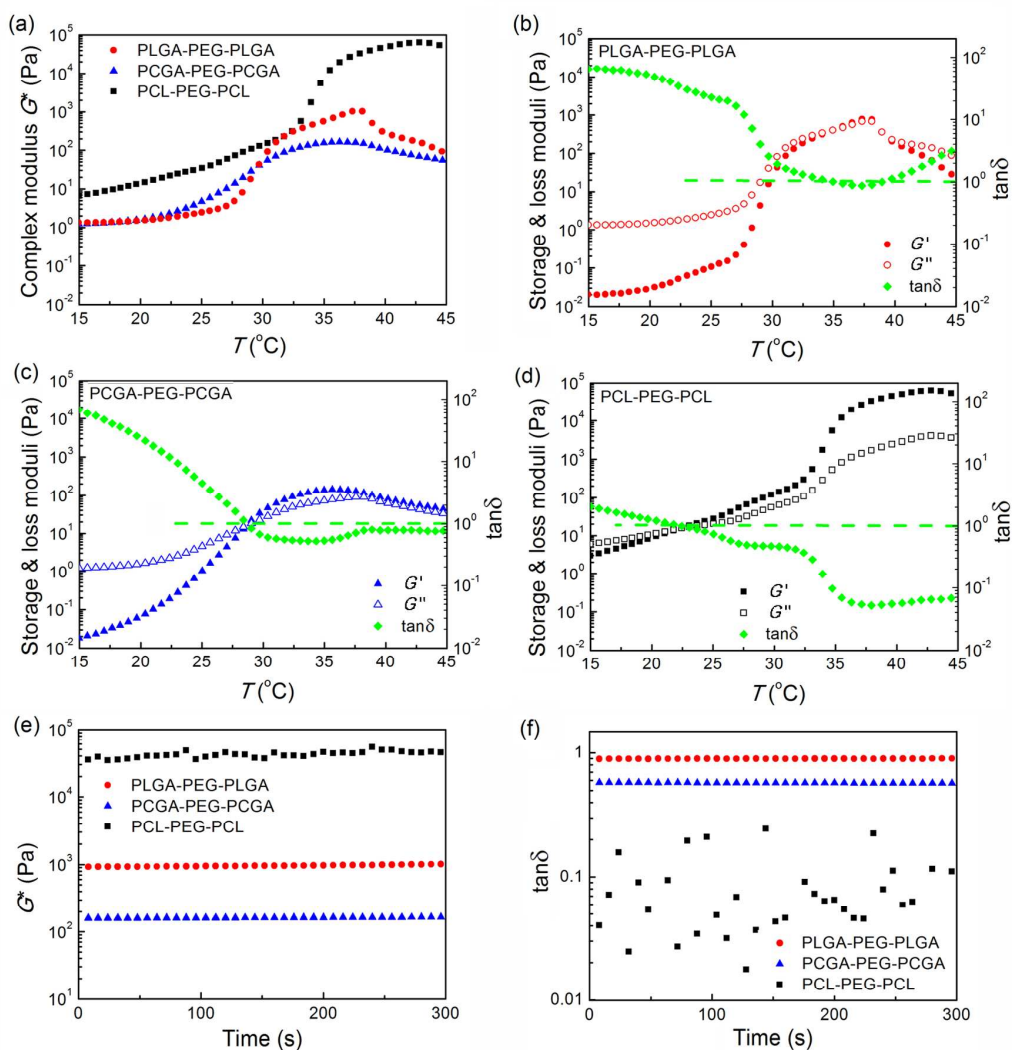


Fig. 6. (a) Complex modulus (G^*) of the indicated three triblock copolymers in NS as

a function of temperature. Heating rates: 0.5 °C/min; oscillatory frequency: 10 rad/s. (b-d) Corresponding storage modulus G' , loss modulus G'' and the tangent of the phase angle $\tan\delta$ of the indicated triblock copolymers in NS as a function of temperature. The dashed lines represent $\tan\delta = 1$, where the effect of viscoelasticity was the most significant. (e-f) Time dependence of G^* and $\tan\delta$ of the indicated thermogels with a frequency of 10 rad/s at a given temperature (37 °C). Polymer concentrations in all of cases were 25 wt%.

Their G^* values exhibited different orders of magnitude at the physiological temperature among the three samples (**Fig. 6e**). The G^* of PCL-PEG-PCL was the highest, and that of PCGA-PEG-PCGA was the smallest. In contrast, the phase angle δ obeyed the order of PLGA-PEG-PLGA > PCGA-PEG-PCGA > PCL-PEG-PCL, and all of those values at 37 °C were less than 45° or $\tan\delta < 1$ as seen in **Fig. 6f**.

***In vivo* evaluation of prevention of abdominal adhesions**

A model of sidewall defect and bowel abrasion in rabbits was used to create peritoneal intestinal adhesions. **Fig. 7** shows the process of establishment of animal model (a-c) and administration of the thermogel (d). The animals in the control group were not treated with any barrier substance on the defect after surgery; the thermogels or CHS solution was painted on the injured sites in the other groups. Compared with the CHS solution, the more viscous thermogels adhered to the defects easily.

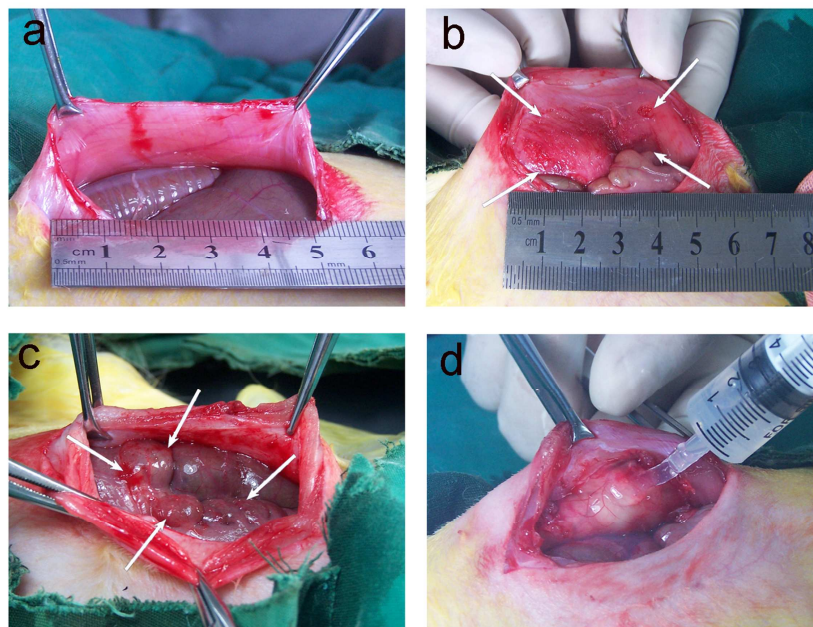


Fig. 7. Photographs of experimental procedure of creating post-surgical peritoneal adhesions in a rabbit model. (a) The enterocoelia of a rabbit was opened. (b) A defect ($4 \times 3 \text{ cm}^2$) comprising the peritoneum and a layer of muscle ($\sim 1 \text{ mm}$ thickness) was created locating 1 cm from the midline of peritoneal wall. (c) The corresponding site on bowel was abraded via a surgical brush resulting in bleeding. (d) The defect was covered by thermogel. Arrows are used to display the defect boundaries.

After surgery for one month, all the animals were euthanized and the autopsy was carried out to determine the abdominal adhesions. The gross inspection did not show any noticeable PLGA-PEG-PLGA and PCGA-PEG-PCGA polymer gels. In contrast, some PCL-PEG-PCL gel residues were observed around the adhesion tissues in a part of animals, as typically illustrated in **Fig. 8**.

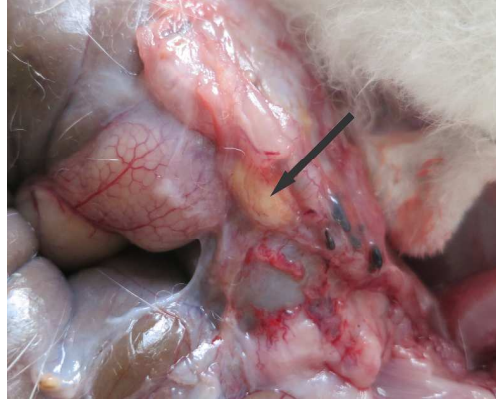


Fig. 8. PCL-PEG-PCL residual was detected at the application site one month after surgery. The arrow indicates the residual PCL-PEG-PCL thermogel.

The efficacies of thermogel against adhesion were evaluated based on the acknowledged protocol.^{30, 31} **Fig. 9a** shows the visual results of abdominal adhesion with various adhesion tenacities, and the percentage of animals with each adhesion score in all the groups is presented in **Fig. 9b**. The control group without any treatment suffered from severe abdominal adhesions, and score 3 adhesions developed in 83% of animals. The administration of PLGA-PEG-PLGA and PCGA-PEG-PCGA thermogels markedly decreased abdominal adhesions. Especially, with the use of PLGA thermogel, adhesions were completely prevented in 50% of tested rabbits, and the injured sites were almost healed within one month; the remaining 50% of animals just suffered from mild intestinal adhesion.

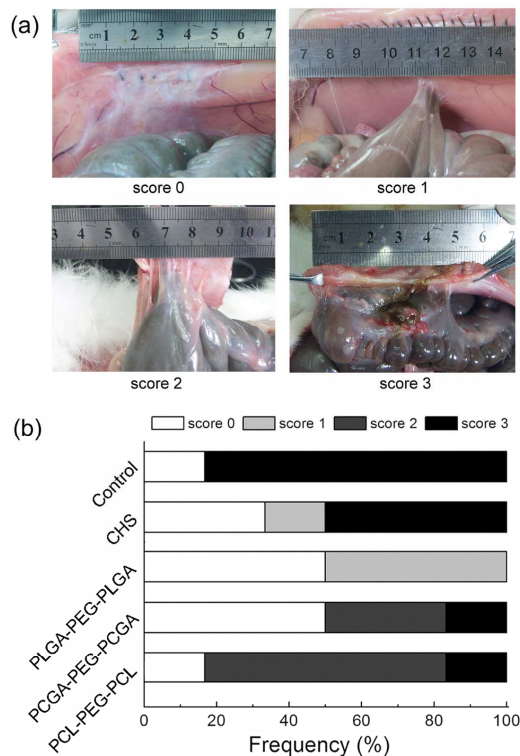


Fig. 9. (a) Photographs of gross observations of the adhesion of defected tissues after one month. The scores demote adhesion tenacity. Score 0: no adhesion; score 1: mild intestinal adhesion and separation was facile; score 2: moderate intestinal adhesion and blunt dissection was needed; score 3: severe intestinal adhesion and sharp dissection was needed. (b) Distribution of adhesion tenacity scores of rabbits treated with the indicated thermogels.

The anti-adhesion efficacy was also quantified via measurement of adhesion areas. The scores of adhesion extent and statistical results of the adhered area are displayed in **Fig. 10**. PLGA-PEG-PLGA and PCGA-PEG-PCGA thermogels significantly reduced both adhesion scores and area, and their adhesion area was statistically different from that of the control group. The adhesion area for PCL-PEG-PCL gel and

CHS solution were slightly lower than that of the control group but no statistically difference was observed.

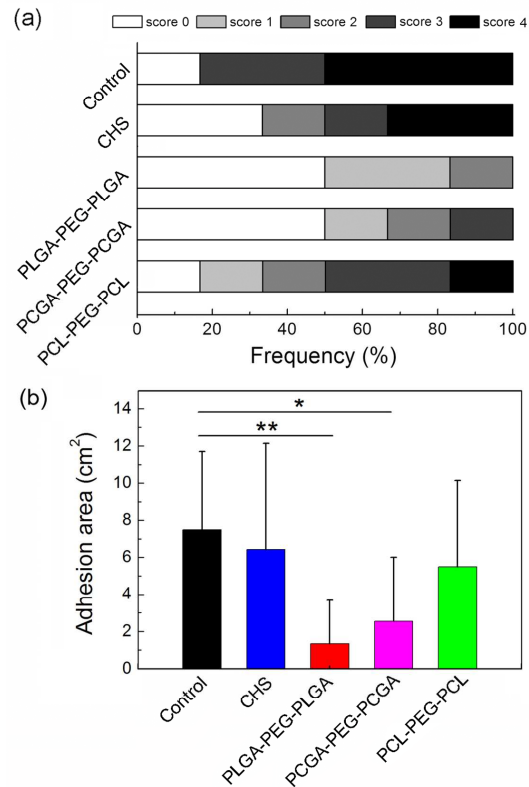


Fig. 10. (a) Distribution of adhesion-scope scores of rabbits treated with the indicated thermogels. Score 0: no adhesion; score 1: adhesion area is between 0-25% of the area of initial abrasion damage; score 2: 25-50% of the area of initial abrasion damage; score 3: 50-75% of the area of initial abrasion damage; score 4: 75-100% of the area of initial abrasion damage. The area of initial abrasion damage was 12 cm². (b) Statistic results of adhesion area of defect in the abdominal wall. “*”: $p < 0.05$; “***”: $p < 0.01$.

Histological observations of the sites of injury were further examined. The surface of the peritoneal defects was completely covered with new mesotheliums in animals

without post-operative adhesions (**Fig. 11a**). Meanwhile, the healed tissue was similar to the normal peritoneal tissue.³ In contrast, specimens suffered from tissue adhesions displayed close apposition of the smooth muscle layers of the bowel to the abdominal wall musculature with different thickness of connected tissue (**Fig. 10c-d**), which reflected the adhesion tenacity as shown in **Fig. 9a**.

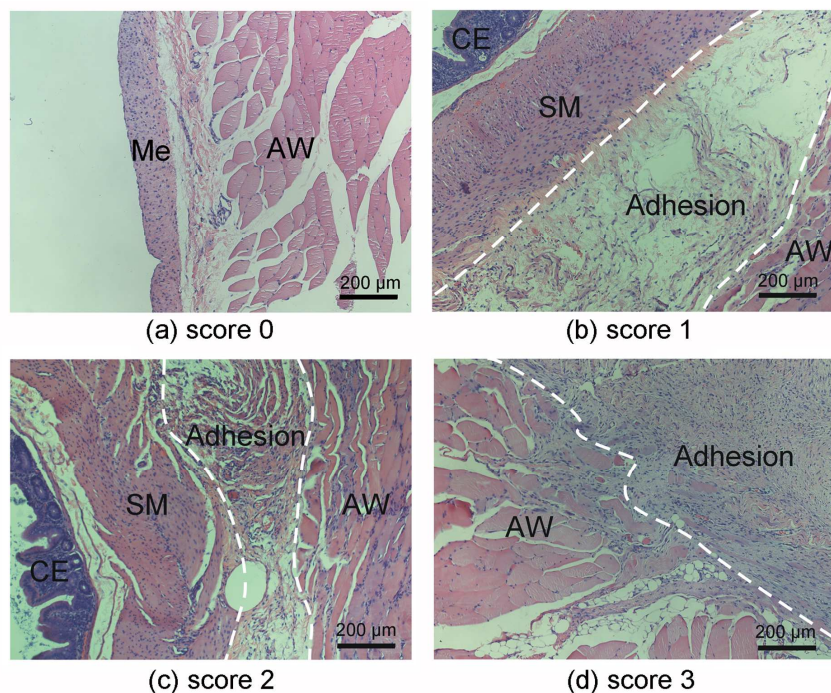


Fig. 11. Histological examination of (a) a healed peritoneal surface, (b) a mild abdominal adhesion, (c) a moderate abdominal adhesion, (d) a severe abdominal adhesion. The scores denote adhesion tenacity. Me: mesothelial layer; CE: cecal mucosa; SM: visceral smooth muscle; AW: abdominal wall.

Discussion

Peritoneal adhesion is one of the principal causes of post-surgical morbidity and mortality.¹⁻³ Barrier devices such as viscous polymer solutions, solid membranes and

in situ-forming hydrogels have been designed to physically separate injured tissue surfaces and thus reduce the contact between affected organs to prevent adhesions.⁹⁻¹² Polymer solutions are faced with the short duration at the application site; solid membranes were hard to complete coverage of damaged tissues; in situ chemical hydrogels triggered by *in vivo* chemical reactions might bring with biocompatibility problems. These disadvantages reduced their efficacies and thus limited their applications. Therefore, an ideal barrier should not only provide complete coverage of the traumatized surfaces, maintain effective during peritoneal healing, but also be biocompatible, biodegradable and conveniently administrated via laparoscope and open surgical procedures.

Thermogelling polymers have great potentials as novel barrier devices for preventing abdominal adhesions. In this study, three polyester-PEG-polyester triblock copolymers with different polyester compositions were synthesized; and their efficacies of prevention of abdominal adhesion were assessed for the first time. These polymers were dissolved in water and formed micelles at low or ambient temperature.^{47, 51, 52} The hydrophilic PEG block is mainly located in the corona of micelle, and the hydrophobic polyester block occupies the core. As the temperature increases, spontaneously physical gelation occurs due to the formation of a percolated micelle network via the micellar aggregation.^{40, 51, 52}

The process of fibrinous adhesion, fibroblasts invasion and collagen deposition play critical roles in adhesion formation.⁵⁴ It is well-known that PEG is a famous anti-adhesion agent against proteins and cells including fibroblasts.⁶¹⁻⁶³ The

thermogels used here were formed via the micellar aggregation and their surfaces were evidently rich of the PEG blocks, resulting in an enhancement of the hydroflotation effect and thus excellent anti-adhesion efficacies.

As comparison between the thermogelling samples is concerned, these thermogels exhibited different gel moduli at the body temperature with the sequence of PCL-PEG-PCL > PLGA-PEG-PLGA > PCGA-PEG-PCGA (**Fig. 6e**). The efficacy of prevention of abdominal adhesions did not follow this sequence. From the animal experiments, PLGA-PEG-PLGA was the best, and PCL-PEG-PCL was the least. This finding suggested that gel strength was not the crucial element as a physical barrier system. On the other hand, the phase angle in **Fig. 6f** followed the same sequence as that of the anti-adhesion efficacy. It seems worthy of noting that larger phase angle does not necessarily lead to more significant anti-adhesion. The phase angle measures the phase lag between stress and strain in a dynamical mechanical experiment. For a full elastic material, $\delta = 0$; for a fully viscous material, $\delta = 90^\circ$; for any viscoelastic material, $\delta \in (0, 90^\circ)$. It could be roughly regarded that $\delta = 45^\circ$ or $\tan\delta = 1$ corresponds to the most significant viscoelastic material. Hence, the ideal phase angle for an excellent anti-adhesion material might be 45° , and PLGA-PEG-PLGA thermogel was very close to this state under the physiological condition.

Besides the hydrophilic surface and the viscoelastic matrix, another important issue comes from the *in vivo* retention time of a material. These thermogels exhibited different degradation periods due to various hydrolysis rates of polyester segment. The *in vivo* persistence of PLGA-PEG-PLGA and PCGA-PEG-PCGA thermogels at

the target sites was only several weeks after the subcutaneous injection into SD rats,⁵¹,⁵⁶ whereas the *in vivo* integrity of PCL-PEG-PCL system at the administration site maintained over many months due to the crystallization of PCL block.⁵⁷ What's more, the enterocoelia is a relative open system and the thermogels were rapidly absorbed at such an administration site.³⁴ The previous studies have also demonstrated that the material residues of barrier devices with prolonged periods at the application sites (over 7 days) could not only negatively affect the remesothelialization of peritoneal defects, but also induce foreign body reactions, resulting in the formation of adhesion.^{11, 64} In this study, no residuals of PLGA-PEG-PLGA and PCGA-PEG-PCGA thermogels were observed at the abdominal space after surgery for one month. Actually, PLGA-PEG-PLGA and PCGA-PEG-PCGA thermogels in the abdominal cavity were completely absorbed within one week (data not shown). On the contrary, residual PCL-PEG-PCL gel was encapsulated as foreign body at the application site (**Fig. 8**). This result further compromised the efficacy of PCL-PEG-PCL system for prevention of post-operative adhesion. A long retention of a barrier device over several weeks might not be helpful for prevention of post-operative abdominal adhesions.

Conclusions

Three thermogelling polyester-PEG-polyester triblock copolymers were tried as physical barrier devices for preventing post-operative peritoneal adhesions in a rabbit model. These polymers were prepared via ring-opening polymerization of commonly

used monomers. Polyester compositions affected their bulk morphology at dry state, and also sol stability and gel modulus in water. All of these thermogels were performed to prevention of post-surgical adhesion. The three thermogels with the same polymer concentration (25 wt%) exhibited different efficacies. PLGA-PEG-PLGA thermogel was the most effective in reducing the formation of intraperitoneal adhesion, whereas PCL-PEG-PCL system presented a little efficacy. Hence, gel modulus at the body temperature was not vital; the viscoelasticity of a gel and its appropriate *in vivo* persistence in the peritoneal cavity played critical roles in prevention of post-surgical adhesions. The present study is meaningful for guiding design of a physical barrier device to prevent post-surgical adhesions.

Acknowledgment

The group was supported by NSF of China (Grants No. 51273217, No. 91127028, No. 81271954, and No. 21034002), Chinese Ministry of Science and Technology (973 Program No. 2011CB606203) and Science and Technology Developing Foundation of Shanghai (Grants No. 12JC1402600, No. 13XD1401000 and No. 12qh1402700).

References

1. M. A. Weibel, G. Majno, *Am J Surg*, 1973, **126**, 345.
2. G. S. Dizerega, *Fertil Steril*, 1994, **61**, 219.
3. Y. Yeo, D. S. Kohane, *Eur J Pharm Biopharm*, 2008, **68**, 57.
4. C. Z. Wei, C. L. Hou, Q. S. Gu, L. X. Jiang, B. Zhu, A. L. Sheng, *Biomaterials*, 2009, **30**, 5534.
5. H. Orita, W. Girgis, G. S. Dizerega, *Drug Dev Res*, 1987, **10**, 97.
6. T. Segura, H. Schmokel, J. A. Hubbell, *J Surg Res*, 2007, **141**, 162.
7. P. N. Zawaneh, S. P. Singh, R. F. Padera, P. W. Henderson, J. A. Spector, D. Putnam, *Proc Natl Acad Sci U S A*, 2010, **107**, 11014.

8. N. Ishiyama, T. Moro, K. Ishihara, T. Ohe, T. Miura, T. Konno, T. Ohyama, M. Kimura, M. Kyomoto, K. Nakamura, H. Kawaguchi, *Biomaterials*, 2010, **31**, 4009.
9. J. M. Burns, K. Skinner, J. Colt, A. Sheidlin, R. Bronson, Y. Yaacobi, E. P. Goldberg, *J Surg Res*, 1995, **59**, 644.
10. J. M. Seeger, L. D. Kaelin, E. M. Staples, Y. Yaacobi, J. C. Bailey, S. Normann, J. W. Burns, E. P. Goldberg, *J Surg Res*, 1997, **68**, 63.
11. S. Matsuda, N. Se, H. Iwata, Y. Ikada, *Biomaterials*, 2002, **23**, 2901.
12. N. M. Paulo, M. Silva, A. M. Moraes, A. P. Rodrigues, L. B. de Menezes, M. P. Miguel, F. G. de Lima, A. D. Faria, L. M. L. Lima, *J Biomed Mater Res Part B*, 2009, **91B**, 221.
13. J. M. Becker, M. T. Dayton, V. W. Fazio, D. E. Beck, S. J. Stryker, S. D. Wexner, B. G. Wolff, P. L. Roberts, L. E. Smith, S. A. Sweeney, M. Moore, *J Am Coll Surg*, 1996, **183**, 297.
14. J. Iliopoulos, G. B. Cornwall, R. O. N. Evans, C. Manganas, K. A. Thomas, D. C. Newman, W. R. Walsh, *J Surg Res*, 2004, **118**, 144.
15. W. R. Walsh, R. O. N. Evans, J. Iliopoulos, G. B. Cornwall, K. A. Thomas, *J Biomed Mater Res Part B*, 2006, **79B**, 166.
16. T. Vermonden, R. Censi, W. E. Hennink, *Chem Rev*, 2012, **112**, 2853.
17. G. T. Chang, T. Y. Ci, L. Yu, J. D. Ding, *J Control Release* 2011, **156**, 21.
18. L. Yu, T. Y. Ci, S. C. Zhou, W. J. Zeng, J. D. Ding, *Biomater Sci*, 2013, **1**, 411.
19. K. Li, L. Yu, X. J. Liu, C. Chen, Q. H. Chen, J. D. Ding, *Biomaterials*, 2013, **34**, 2834.
20. T. Y. Ci, L. Chen, T. Li, G. T. Chang, L. Yu, J. D. Ding, *Biomater Sci*, 2013, **1**, 1235.
21. L. Yu, K. Li, X. J. Liu, C. Chen, Y. C. Bao, T. Y. Ci, Q. H. Chen, J. D. Ding, *J Pharm Sci*, 2013, **102**, 4140.
22. D. Y. Ko, U. P. Shinde, B. Yeon, B. Jeong, *Prog Polym Sci*, 2013, **38**, 672.
23. R. Jin, L. S. M. Teixeira, P. J. Dijkstra, Z. Y. Zhong, C. A. van Blitterswijk, M. Karperien, J. Feijen, *Tissue Eng Part A*, 2010, **16**, 2429.
24. H. K. Kim, W. S. Shim, S. E. Kim, K. H. Lee, E. Kang, J. H. Kim, K. Kim, I. C. Kwon, D. S. Lee, *Tissue Eng Part A*, 2009, **15**, 923.
25. V. X. Truong, M. P. Ablett, H. T. J. Gilbert, J. Bowen, S. M. Richardson, J. A. Hoyland, A. P. Dove, *Biomater Sci*, 2014, **2**, 167.
26. I. Kumano, M. Ishihara, S. Nakamura, S. Kishimoto, M. Fujita, H. Hattori, T. Horio, Y. Tanaka, K. Hase, T. Maehara, *Gastrointest Endosc*, 2012, **75**, 841.
27. L. Yu, W. Xu, W. J. C. Shen, L. P., Y. Liu, Z. S. Li, J. D. Ding, *Acta Biomater*, 2014, **10**, 1251.
28. D. Gyawali, P. Nair, H. K. W. Kim, J. Yang, *Biomater Sci*, 2013, **1**, 52.
29. T. D. Johnson, J. A. DeQuach, R. Gaetani, J. Ungerleider, D. Elhag, V. Nigam, A. Behfar, K. L. Christman, *Biomater Sci*, 2014, DOI: 10.1039/c3bm60283d.
30. Y. Yeo, C. B. Highley, E. Bellas, T. Ito, R. Marini, R. Langer, D. S. Kohane, *Biomaterials*, 2006, **27**, 4698.
31. Y. Yeo, E. Bellas, C. B. Highley, R. Langer, D. S. Kohane, *Biomaterials*, 2007, **28**, 3704.
32. T. Ito, Y. Yeo, C. B. Highley, E. Bellas, D. S. Kohane, *Biomaterials*, 2007, **28**, 3418.
33. J. L. West, J. A. Hubbell, *Biomaterials*, 1995, **16**, 1153.
34. B. Yang, C. Y. Gong, Z. Y. Qian, X. Zhao, Z. Y. Li, X. R. Qi, S. T. Zhou, Q. A. Zhong, F. Luo, Y. Q. Wei, *BMC Biotechnol*, 2010, **10**, 65.
35. Z. Zhang, J. Ni, L. Chen, L. Yu, J. W. Xu, J. D. Ding, *J Biomed Mater Res Part B*, 2012, **100B**, 1599.
36. J. H. Hong, J. W. Choe, G. Y. Kwon, D. Y. Cho, D. S. Sohn, S. W. Kim, Y. C. Woo, C. J. Lee, H. Kang, *J Surg Res*, 2011, **166**, 206.
37. B. Jeong, Y. H. Bae, D. S. Lee, S. W. Kim, *Nature*, 1997, **388**, 860.

38. L. Yu, J. D. Ding, *Chem Soc Rev*, 2008, **37**, 1473.
39. X. J. Loh, S. H. Goh, J. Li, *Biomacromolecules*, 2007, **8**, 585.
40. L. Yu, Z. Zhang, H. Zhang, J. D. Ding, *Biomacromolecules*, 2009, **10**, 1547.
41. C. D. Liu, Z. Zhang, K. L. Liu, X. Ni, J. Li, *Soft Matter*, 2013, **9**, 787.
42. H. J. Moon, D. Y. Ko, M. H. Park, M. K. Joo, B. Jeong, *Chem Soc Rev*, 2012, **41**, 4860.
43. B. Jeong, Y. H. Bae, S. W. Kim, *Macromolecules*, 1999, **32**, 7064.
44. D. S. Lee, M. S. Shim, S. W. Kim, H. Lee, I. Park, T. Y. Chang, *Macromol Rapid Commun*, 2001, **22**, 587.
45. C. Chen, L. Chen, L. P. Cao, W. J. Shen, L. Yu, J. D. Ding, *RSC Adv*, 2014, **4**, 8789.
46. L. Yu, Z. Zhang, J. D. Ding, *Biomacromolecules*, 2011, **12**, 1290.
47. S. J. Bae, J. M. Suh, Y. S. Sohn, Y. H. Bae, S. W. Kim, B. Jeong, *Macromolecules*, 2005, **38**, 5260.
48. J. S. Kwon, S. M. Yoon, D. Y. Kwon, D. Y. Kim, G. Z. Tai, L. M. Jin, B. Song, B. Lee, J. H. Kim, D. K. Han, B. H. Min, M. S. Kim, *J Mat Chem B*, 2013, **1**, 3314.
49. Z. Zhang, Y. X. Lai, L. Yu, J. D. Ding, *Biomaterials*, 2010, **31**, 7873.
50. A. Petit, B. Muller, P. Bruin, R. Meyboom, M. Piest, L. M. J. Kroon-Batenburg, L. G. J. de Leede, W. E. Hennink, T. Vermonden, *Acta Biomater*, 2012, **8**, 4260.
51. L. Yu, W. J. Shen, D. C. Yang, J. D. Ding, *Macromol Res*, 2013, **21**, 207.
52. L. Yu, G. T. Chang, H. Zhang, J. D. Ding, *J Polym Sci, Part A: Polym Chem*, 2007, **45**, 1122.
53. H. Zhang, L. Yu, J. D. Ding, *Macromolecules*, 2008, **41**, 6493.
54. Z. Zhang, J. Ni, L. Chen, L. Yu, J. W. Xu, J. D. Ding, *Biomaterials*, 2011, **32**, 4725.
55. G. M. Zentner, R. Rathi, C. Shih, J. C. McRea, M. H. Seo, H. Oh, B. G. Rhee, J. Mestecky, Z. Moldoveanu, M. Morgan, S. Weitman, *J Control Release*, 2001, **72**, 203.
56. L. Yu, Z. Zhang, H. Zhang, J. D. Ding, *Biomacromolecules*, 2010, **11**, 2169.
57. Y. M. Kang, S. H. Lee, J. Y. Lee, J. S. Son, B. S. Kim, B. Lee, H. J. Chun, B. H. Min, J. H. Kim, M. S. Kim, *Biomaterials*, 2010, **31**, 2453.
58. L. Yu, Z. Zhang, J. D. Ding, *Macromol Res*, 2012, **20**, 234.
59. L. Yu, G. T. Chang, H. Zhang, J. D. Ding, *Int J Pharm*, 2008, **348**, 95.
60. L. Yu, H. Zhang, J. D. Ding, *Angew Chem-Int Edit*, 2006, **45**, 2232.
61. X. Yao, R. Peng, J. D. Ding, *Adv Mater*, 2013, **25**, 5257.
62. X. Wang, C. Yan, K. Ye, Y. He, Z. H. Li, J. D. Ding, *Biomaterials*, 2013, **34**, 2865.
63. C. Yan, J. G. Sun, J. D. Ding, *Biomaterials*, 2011, **32**, 3931.
64. M. Wallwiener, S. Brucker, H. Hierlemann, C. Brochhausen, E. Solomayer, C. Wallwiener, *Fertil Steril*, 2006, **86**, 1266.

For Table of Contents use only

Graphics for TOC

Comparative studies of thermogels in preventing post-operative adhesions and corresponding mechanisms

Lin Yu^{a,1}, Hongtao Hu^{b,1}, Lin Chen^a, Xiaogang Bao^b, Yuzhuo Li^a, Liang Chen^a,

Guohua Xu^{b,}, Xiaojian Ye^b, Jiandong Ding^{a,*}*

Thermogelling PLGA-PEG-PLGA, PCGA-PEG-PCGA, and PCL-PEG-PCL triblock copolymers and their efficacies of prevention of post-surgical peritoneal adhesions in rabbits were investigated and compared.

